



# Interferometric Probes of Many-Body Localization

The Harvard community has made this article openly available. [Please share](#) how this access benefits you. Your story matters

Citation	Serbyn, M., M. Knap, S. Gopalakrishnan, Z. Papić, N. Y. Yao, C. R. Laumann, D. A. Abanin, M. D. Lukin, and E. A. Demler. 2014. "Interferometric Probes of Many-Body Localization." Physical Review Letters 113 (14) (October). doi:10.1103/physrevlett.113.147204.
Published Version	doi:10.1103/PhysRevLett.113.147204
Citable link	<a href="http://nrs.harvard.edu/urn-3:HUL.InstRepos:16914859">http://nrs.harvard.edu/urn-3:HUL.InstRepos:16914859</a>
Terms of Use	This article was downloaded from Harvard University's DASH repository, and is made available under the terms and conditions applicable to Other Posted Material, as set forth at <a href="http://nrs.harvard.edu/urn-3:HUL.InstRepos:dash.current.terms-of-use#LAA">http://nrs.harvard.edu/urn-3:HUL.InstRepos:dash.current.terms-of-use#LAA</a>

## Interferometric Probes of Many-Body Localization

M. Serbyn,<sup>1</sup> M. Knap,<sup>2,3</sup> S. Gopalakrishnan,<sup>2</sup> Z. Papić,<sup>4,5</sup> N. Y. Yao,<sup>2</sup> C. R. Laumann,<sup>2,4,6</sup>  
D. A. Abanin,<sup>4,5</sup> M. D. Lukin,<sup>2</sup> and E. A. Demler<sup>2</sup>

<sup>1</sup>*Department of Physics, Massachusetts Institute of Technology, Cambridge, Massachusetts 02139, USA*

<sup>2</sup>*Department of Physics, Harvard University, Cambridge, Massachusetts 02138, USA*

<sup>3</sup>*ITAMP, Harvard-Smithsonian Center for Astrophysics, Cambridge, Massachusetts 02138, USA*

<sup>4</sup>*Perimeter Institute for Theoretical Physics, Waterloo, Ontario N2L 2Y5, Canada*

<sup>5</sup>*Institute for Quantum Computing, Waterloo, Ontario N2L 3G1, Canada*

<sup>6</sup>*Department of Physics, University of Washington, Seattle, Washington 98195, USA*

(Received 13 March 2014; revised manuscript received 17 August 2014; published 3 October 2014)

We propose a method for detecting many-body localization (MBL) in disordered spin systems. The method involves pulsed coherent spin manipulations that probe the dephasing of a given spin due to its entanglement with a set of distant spins. It allows one to distinguish the MBL phase from a noninteracting localized phase and a delocalized phase. In particular, we show that for a properly chosen pulse sequence the MBL phase exhibits a characteristic power-law decay reflecting its slow growth of entanglement. We find that this power-law decay is robust with respect to thermal and disorder averaging, provide numerical simulations supporting our results, and discuss possible experimental realizations in solid-state and cold-atom systems.

DOI: 10.1103/PhysRevLett.113.147204

PACS numbers: 75.10.Jm, 05.70.Ln, 67.85.-d, 72.15.Rn

**Introduction.**—One of the central assumptions of statistical mechanics, which underlies conventional kinetic and transport theories, is that interactions between particles establish local equilibrium. This assumption, however, was recently shown to fail in a class of disordered interacting systems [1–22]. If the disorder is strong enough, it can give rise to a many-body localized (MBL) phase, in which transport is absent and the system cannot act as a heat bath for its constituent parts. Although the MBL phase resembles a conventional noninteracting Anderson insulator in that diffusion is absent, it has very different dynamical properties. Specifically, interactions between particles in the MBL phase can cause dephasing and can generate long-range entanglement, leading to the slow growth of entanglement entropy [8,9,11–13].

Experimental investigations of MBL in conventional solid-state systems [23] are challenging, as these systems are strongly coupled to the environment [21], e.g., due to the presence of phonons. However, recent experimental advances have resulted in the realization of isolated synthetic many-body systems with tunable interactions and disorder, which constitute promising platforms to explore MBL. Such systems include ultracold atoms in optical lattices [24–26], polar molecules [27,28], and isolated spin impurities in solids [29]. Although conventional transport experiments are challenging in these systems, they often allow for the precise manipulation of individual degrees of freedom to characterize their quantum evolution. This motivates the development of new approaches for detecting and exploring the MBL phase.

In this Letter, we propose and analyze a new method for studying MBL, based on coherent manipulation of individual degrees of freedom. We focus on disordered spin systems, and show that spin-echo type measurements

performed on individual spins can be used as sensitive probes of localization [Figs. 1(a)–1(c)]. Such measurements are standard in bulk liquid and solid-state spin systems (see [30] and references therein), and have recently been extended to probe many-body physics [19,31–34].

Specifically, in order to probe MBL, we introduce a modified nonlocal spin-echo protocol [Fig. 1(c)], akin to the double electron-electron resonance (DEER) technique in electron spin resonance [35–37], that allows one to probe the dynamical correlations between remote regions of a many-body system. This approach can reveal interaction effects and probe quantum entanglement within the MBL phase. In particular, the slow growth of entanglement entropy associated with the MBL phase manifests itself in a power-law decay of the DEER response. Furthermore, by measuring both the spin-echo and DEER response one can distinguish the MBL phase from a noninteracting localized phase as well as a diffusive phase [Fig. 1(d)]. We discuss specific realizations of our proposal in several cold-atom and solid-state systems.

**Approach.**—The key idea of this Letter can be illustrated using a phenomenological model of the MBL phase [12,13] that characterizes it by an infinite number of local integrals of motion, which can be chosen as effective spin-1/2 operators  $\tau_i^z$  with eigenvalues  $\pm 1$ . In terms of these variables, the MBL Hamiltonian is [12,13]

$$\hat{H} = \sum_i \tilde{h}_i \tau_i^z + \sum_{ij} \mathcal{J}_{ij} \tau_i^z \tau_j^z + \sum_{ijk} \mathcal{J}_{ijk} \tau_i^z \tau_j^z \tau_k^z + \dots \quad (1)$$

The couplings  $\mathcal{J}_{ij}, \mathcal{J}_{ijk}, \dots$  fall off exponentially with separation with a characteristic localization length  $\xi$  (expressed in units of the lattice constant). The Hamiltonian (1) conserves the expectation value of each  $\tau_i^z$ ; however, interactions between effective spins randomize relative phases of different components of the wave function.

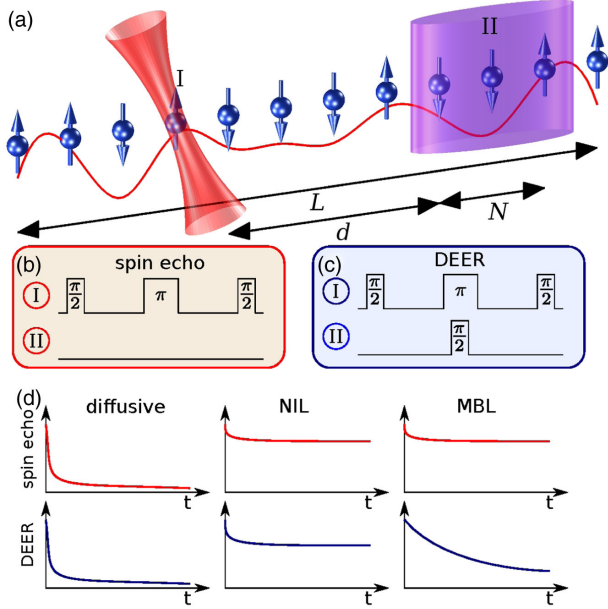


FIG. 1 (color online). Schematic illustration of the proposed protocols. (a) Spins are manipulated with lasers in two spatially separated regions I and II. (b) A Hahn spin-echo sequence is applied to region I while leaving region II untouched. (c) The DEER protocol differs by  $\pi/2$  rotations in region II which are performed after half of the evolution time. Both protocols work for arbitrary initial states (product states, thermal state, etc.). (d) Schematic response of a system in the diffusive (left), noninteracting localized (center), and many-body localized (right) phases, to spin-echo and DEER protocols, respectively. The combined information from both sequences allows one to distinguish the different phases.

Such dephasing generates entanglement between distant parts of the system [12,13].

We first discuss interferometric signatures of Hamiltonian (1) assuming that one can directly manipulate the effective spins  $\tau_i^z$  (in what follows we shall refer to effective spins simply as “spins”), and later we generalize these arguments to realistic cases involving manipulation of physical, rather than effective, spins.

Let us first consider a simple spin-echo sequence applied to an individual spin I [Fig. 1(b)]. We start from an arbitrary eigenstate of  $\hat{H}$  (i.e., a product state of the form  $|\uparrow\downarrow\uparrow\downarrow\downarrow\dots\rangle$ ) and perform thermal averaging later. We initialize spin I in a superposition state  $|+\rangle_I = (|\uparrow\rangle_I + |\downarrow\rangle_I)/\sqrt{2}$ . Spin I precesses in the magnetic field  $h_{\text{eff}}(\mathbf{I}) = \tilde{h}_I + \sum_j \mathcal{J}_{Ij} \tau_j^z + \sum_{j,k} \mathcal{J}_{Ijk} \tau_j^z \tau_k^z + \dots$ , which depends on the state of the surrounding spins. The thermal average over initial states gives rise to dephasing and decay of the free precession signal. The standard spin-echo sequence, however, allows one to recover the quantum coherence of spin I by applying a time-reversal  $\pi$  pulse to it at time  $t/2$ . For the MBL Hamiltonian (1), the precession induced by  $h_{\text{eff}}(\mathbf{I})$  over the initial evolution for  $t/2$  is canceled by the precession accumulated during evolution for time  $t/2$  after the  $\pi$  pulse, independent of the value of  $h_{\text{eff}}(\mathbf{I})$ . However, since spin

echo is insensitive to dephasing in the MBL phase, it does not distinguish between noninteracting and MBL phases.

We next introduce a modified spin-echo protocol, which directly probes interaction effects in the MBL phase. The idea is to perturb spins in a remote region II, situated at a distance  $d \gtrsim \xi$  away from I, halfway through the spin-echo sequence. More specifically, DEER is identical to spin echo for the first  $t/2$  of the time evolution, but simultaneously with the  $\pi$  pulse to spin I, another pulse (which we shall take to be a  $\pi/2$  pulse) is applied to all the spins in region II. Assuming that the remaining spins are in a state with definite  $\tau^z$ , all interactions except those between spin I and region II are decoupled by this protocol; thus, the decay of the DEER response directly measures the influence of region II on spin I.

Before analyzing the DEER response, we summarize our qualitative expectations [Fig. 1(d)]. In the diffusive phase, both the spin-echo and DEER responses should decay on a fast time scale set by the spin-spin interaction. In the noninteracting localized phase, both the spin-echo and DEER responses should saturate at the same nonzero value in the thermodynamic limit, as dephasing is absent. Finally, in the MBL phase, the spin-echo response should saturate while the DEER response exhibits slow decay.

*DEER response.*—The time evolution of the many-body wave function under the DEER sequence is described by

$$|\psi(t)\rangle = R_I^{\pi/2} e^{-i\hat{H}t/2} R_I^\pi R_{II}^{\pi/2} e^{-i\hat{H}t/2} R_I^{\pi/2} |\psi(0)\rangle, \quad (2)$$

where  $R_r^{\pi/2} = \prod_{j \in r} (\hat{1} - i\delta_j^y)/\sqrt{2}$ , and  $R_r^\pi = (R_r^{\pi/2})^2$ .

Many features of the DEER response can be understood by keeping only two-spin interactions in Eq. (1), in which case the response takes a compact form,

$$\mathcal{D}(t) \equiv \langle \psi(t) | \hat{\tau}_I^z | \psi(t) \rangle = \text{Re} \prod_{j \in \text{II}} [(1 + e^{2i\mathcal{J}_{Ij}\tau_j^z t})/2], \quad (3)$$

where the product is over the  $N$  spins of region II and  $\tau_j$  is the initial configuration of spin  $j$ . The additional effects induced by three- and higher-spin interactions are considered below; see also the Supplemental Material [38].

To analyze the behavior of  $\mathcal{D}(t)$ , we note that the couplings  $\mathcal{J}_{Ij}$  decay exponentially with the separation  $|j - I|$ , and therefore different terms on the rhs of Eq. (3) oscillate at very different frequencies. This leads to a separation of scales: at a given time, there are  $\sim N_{\text{fast}}$  “fast” coupling constants, for which  $\mathcal{J}_{Ij} t \gg 1$ , and the remaining ones are “slow,” i.e.  $\mathcal{J}_{Ij} t \ll 1$ . In the product in Eq. (3), the terms corresponding to slow couplings contribute factors which are close to 1 and are nearly time independent, while the terms corresponding to fast couplings oscillate between 0 and 1. Thus,  $\mathcal{D}(t)$  can be separated into a time-averaged term  $\bar{\mathcal{D}}(t)$  and an oscillatory term  $\mathcal{D}_{\text{osc}}(t)$ ,

$$\mathcal{D}(t) = \bar{\mathcal{D}}(t) + \mathcal{D}_{\text{osc}}(t), \quad \bar{\mathcal{D}}(t) = 1/2^{N_{\text{fast}}(t)}, \quad (4)$$

where the first term is obtained by replacing rapidly oscillating terms with their average value of 1/2.

The number of fast couplings depends on time, and can be estimated knowing that  $\mathcal{J}_{Ij} \propto \exp(-|j - I|/\xi)$ . A

coupling becomes fast when  $|j - I| \lesssim \xi \log(t)$ , i.e., when entanglement has had time to propagate between the two regions [11]. Thus, the DEER response has three regimes: (i) at short times  $t \lesssim t_0 \equiv \hbar/J_{Ik}$  (where  $k = I + d$  is the spin in region II that is most strongly coupled to I),  $N_{\text{fast}} = 0$  and dephasing is absent; (ii) at intermediate times  $t_0 \lesssim t \lesssim t_0 e^{N/\xi}$ , we find  $N_{\text{fast}}(t) \sim \xi \log(t/t_0)$ , so that  $\bar{D}(t) \sim t^{-\xi \ln 2}$ ; and (iii) at very long times  $t \gg t_0 e^{N/\xi}$ , all couplings are fast, so that the DEER response saturates at  $\bar{D}(\infty) \approx 2^{-N}$ . These three regimes can be combined using the following interpolation formula:

$$\bar{D}(t) = \begin{cases} (1 + t^2/t_0^2)^{-\alpha/2} & t \lesssim t_0 e^{N/\xi} \\ 2^{-N} & t \gg t_0 e^{N/\xi}, \end{cases} \quad (5)$$

where  $\alpha = \xi \ln 2$ . Upon disorder averaging, one expects  $\mathcal{D}_{\text{osc}}(t)$  to be suppressed, as the oscillation frequencies vary randomly from realization to realization. Thus the full disorder-averaged DEER response is given by Eq. (5).

We note that, although truncating Eq. (1) at two-spin interactions gives the correct structure for the time- and disorder-averaged DEER response, it leads to incorrect predictions for the oscillatory term  $\mathcal{D}_{\text{osc}}(t)$ . Three- and higher-spin terms make the oscillation frequencies dependent on the initial eigenstate, leading to the suppression of  $\mathcal{D}_{\text{osc}}(t)$  upon thermal averaging (see [38] for details).

*Numerical simulations.*—We now test the previous arguments against numerical simulations by studying the spin-echo fidelity and DEER response for a 1D random-field XXZ spin chain, believed to exhibit an MBL phase [6],

$$\hat{H} = (J_{\perp}/2) \sum_{\langle ij \rangle} (\hat{S}_i^+ \hat{S}_j^- + \hat{S}_j^+ \hat{S}_i^-) + J_z \sum_{\langle ij \rangle} \hat{S}_i^z \hat{S}_j^z + \sum_i h_i \hat{S}_i^z, \quad (6)$$

where  $\hat{S}_j$  are spin-1/2 operators with eigenvalues  $\pm 1/2$ ,  $\hat{S}_j^{\pm} = \hat{S}_j^x \pm i \hat{S}_j^y$ , and the random field  $h_i$  is uniformly distributed in the interval  $[-W; W]$ . For open boundary conditions and  $J_z = 0$ ,  $\hat{H}$  maps onto free fermions moving in a disorder potential. In this limit, the system is in a noninteracting localized phase for any  $W > 0$ . When  $J_z \neq 0$ , the system is believed to exhibit both MBL and delocalized phases as a function of  $W/J_{\perp}$  [6].

Although the Hamiltonian in the MBL phase can be expressed in the form of Eq. (1) when written in the basis of conserved quantities (effective spins), in experiments one manipulates the physical  $S$  spins, rather than the effective  $\tau$  spins. In what follows, we calculate the response for spin-echo and DEER protocols performed on the physical spins. We show that, due to the local relation between physical and effective spin operators, the behavior of the spin-echo and DEER responses discussed above remains qualitatively correct throughout the MBL phase, and becomes quantitatively correct in the limit of strong disorder.

We study time evolution and response functions by exact diagonalization of the Hamiltonian (6). Unless otherwise

specified, the chain contains  $L = 12$  spins with open boundary conditions. The Hamiltonian is diagonalized for all total  $S^z$  sectors, and the DEER response  $\mathcal{D}(t) \equiv \langle \psi(t) | \hat{S}_I^z | \psi(t) \rangle$  is calculated numerically. We consider mixed initial states by choosing  $|\psi(0)\rangle$  as a random eigenstate satisfying  $\mathcal{D}(0) > 0$ , and by performing thermal averaging over the entire band (infinite temperature), denoted by single brackets,  $\langle \mathcal{D}(t) \rangle$ . Our results also hold when the system is initialized in a product state [38].

We first calculate the spin-echo and DEER response for a single disorder realization with  $W = 6$  in Fig. 2(a) [39]. Thermal averaging is performed over 50 random eigenstates and  $J_z = J_{\perp}$ . The spin-echo response  $\mathcal{F}(t)$  quickly saturates and remains of order 1. In contrast, the DEER response  $\mathcal{D}(t)$  decays to a value much smaller than 1. The saturation value of  $\mathcal{F}(t)$  [Fig. 2(b)] is generally less than 1 due to the difference between physical and effective spins. As each pulse affects several effective spins, the probability of return to the initial state at the end of the sequence is reduced.

Figure 3 demonstrates that  $\mathcal{D}(t)$ , thermally averaged over 50 eigenstates for a single-disorder realization at  $W = 6$ , fits well to the modified interpolation formula of Eq. (5),  $\mathcal{D}(t) = A/(1 + t^2/t_0^2)^{\alpha/2}$ , where we have introduced a multiplier  $A$  to account for the difference between effective and physical spins. In this example, spin I is located at  $I = 3$ , and separated by  $d = 3$  spins from region II with  $N = 7$  spins. Agreement with the general trend in Eq. (5), despite the presence of significant oscillations from  $\mathcal{D}_{\text{osc}}$ , may be useful for potential experiments in which the disorder cannot be easily varied.

Finally, performing both thermal and disorder averaging of the DEER response [denoted by  $\langle\langle \mathcal{D}(t) \rangle\rangle$ ] reveals a clear power-law decay spanning several decades, Fig. 4(a). Results are obtained for XXZ model with both weak ( $J_z = 0.1J_{\perp}$ ) and moderate ( $J_z = J_{\perp}$ ) interactions, and both small ( $d = 3$ ) and large ( $d = 7$ ) separations between spin I and region II. Power-law decay, shown on a double logarithmic scale, is present in all cases, while different values of  $d$  suggest the exponential sensitivity of  $t_0 [\sim \exp(d/\xi)]$  confirmed by additional studies (not shown). The disorder strength is  $W = 8J_{\perp}$ , and the size of region II is  $N = 3$ .

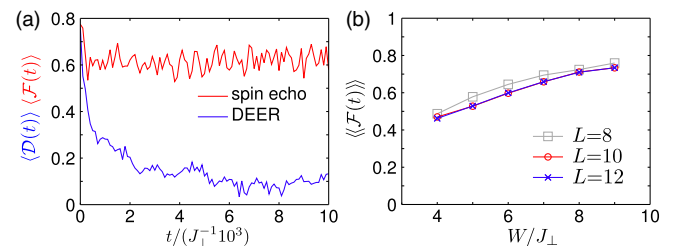


FIG. 2 (color online). (a) Typical behavior of thermally averaged spin-echo  $\mathcal{F}(t)$  and DEER response  $\mathcal{D}(t)$  for the random-field XXZ model [Eq. (6)] and a single disorder realization ( $W = 6$ ).  $\mathcal{D}(t)$  slowly decays, while  $\mathcal{F}(t)$  quickly saturates. (b) Disorder-averaged  $\mathcal{F}(t)$  saturates to a nonzero value in thermodynamic limit, and approaches 1 for strong disorder  $W$ .

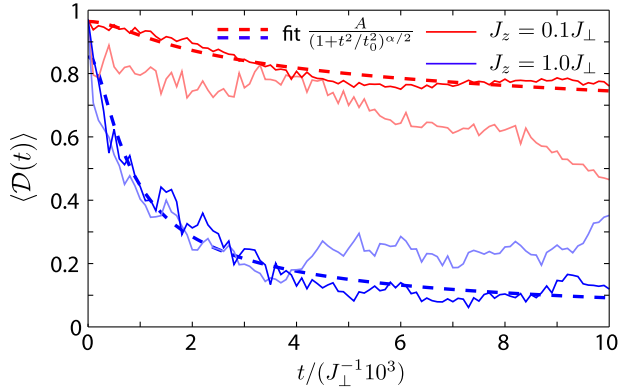


FIG. 3 (color online). Thermally averaged DEER response at weak interactions ( $J_z = 0.1J_{\perp}$ ) and moderate interactions ( $J_z = J_{\perp}$ ) in the XXZ model. In both cases, we show two particular disorder realizations. Despite strong sample-to-sample fluctuations, the response is consistent with Eq. (5).

Figure 4(b) shows the dependence of the exponent governing the power-law decay,  $\alpha$ , on disorder, for  $d = 7$  and  $N = 3$ . Exponent  $\alpha$  decreases with  $W$ , and is well described by the functional form  $\alpha = c_1/\ln(c_2W)$ , consistent with the relation  $\alpha = \xi \ln 2$  and scaling of the localization length  $\xi \propto 1/\ln(W)$  at strong disorder.

The dependence of the saturated value  $\langle\langle \mathcal{D}(\infty) \rangle\rangle$  on the number of spins  $N$  in region II is presented in Fig. 4(c). The saturation value, which is nearly independent of the

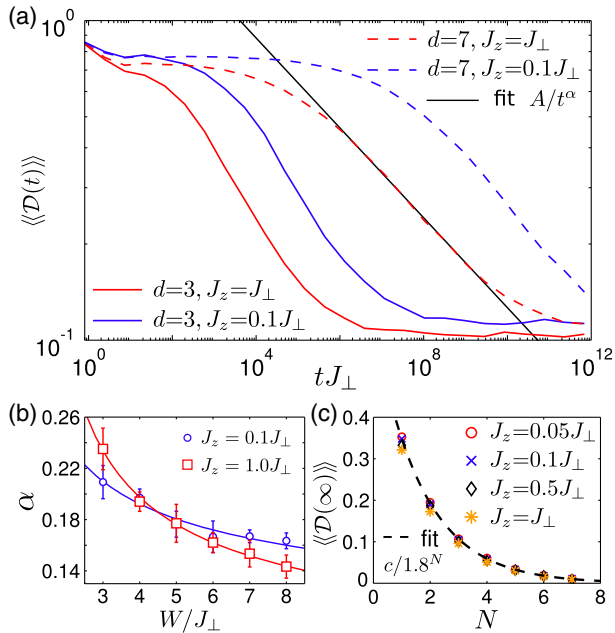


FIG. 4 (color online). (a) DEER response, after thermal and disorder averaging, for different values of the interaction  $J_z$  and separations  $d$  between spin I and region II. Power-law decay of the response, spanning multiple decades, can be seen in all cases. (b) Exponent of the power law,  $\alpha$ , scales as  $\alpha = c_1/\ln(c_2W)$  with disorder  $W$ , consistent with  $\alpha = \xi \ln 2$  and the scaling of the localization length,  $\xi \sim 1/\ln(W)$ , at strong disorder. (c) Saturated DEER response as a function of size of region II (denoted  $N$ ) decreases as  $c/1.8^N$ , and is insensitive to interaction  $J_z$ .

interaction strength, fits to a function  $f(k) = c/1.8^N$  [for effective spins, by contrast, Eq. (5) predicts  $1/2^N$ ]. Thus, the DEER response for physical spins has the same functional form as for the effective spins but with a different coefficient, due to the difference between physical and effective spin operators.

*Experimental considerations.*—Promising experimental systems for studying MBL include ultracold atomic [24–26] and molecular [27,28] gases confined in optical lattices, as well as localized spin defects in solids such as nitrogen-vacancy (NV) centers in diamond [29]. Such systems can be well isolated from their environment and can feature long coherence times. Further, they can be manipulated by optical and microwave fields, thus allowing for implementation of the pulsed protocols. We now evaluate the feasibility of the present protocols in a number of experimental settings. In each case, the slow DEER decay can be observed provided that (a) there exists a separation of scales between the couplings  $J_{\perp}, J_z$  and the extrinsic decoherence rate  $T_1^{-1}$  and (b) excitations are localized on a small number of sites, ensuring a reasonable spin-echo fidelity.

The most direct implementation of our protocols involves a two-component Fermi- or Bose-Hubbard model in a disordered optical lattice; in such models, random spin-spin interactions arise via superexchange, and random fields can be imposed via a state-dependent optical lattice. The typical interaction scale  $J \approx 10$  Hz, whereas achievable  $T_1$  times limited by particle loss are about 10 s [40–42]. The ratio between these scales is  $\lesssim 500$ ; thus, the DEER protocol can detect entanglement at realistic distances  $\lesssim \xi \ln(JT_1) \approx 6\xi$ . Even more favorable conditions exist in systems with dipolar interactions. For instance, in NV-center samples at achievable densities (e.g., spacings of 10 nm),  $J \sim 100$  kHz and  $T_1 \sim 10$  ms, yielding  $T_1/J^{-1} \sim 5 \times 10^3$ . For Rydberg atoms,  $J \sim (1-10)$  MHz (e.g., in 38s state of Rb at typical distances  $\approx 5 \mu\text{m}$ ), while  $T_1 \sim 100 \mu\text{s}$ ; therefore,  $T_1/J^{-1} \sim (0.5-5) \times 10^3$ . Finally, for polar molecules in optical lattices,  $J \sim 50$  Hz and  $T_1 \sim 25$  s, and thus  $T_1/J^{-1} \sim 8 \times 10^3$ . For all these cases, therefore, it should be feasible to probe interaction effects in the MBL phase through DEER; however, the functional form of the dephasing might differ from that considered here, as the power-law tails of the dipolar interactions affect localization (although the MBL phase is expected to survive for dipolar interactions in one dimension [43–45]).

Before concluding, we note that since the proposed protocols can distinguish various phases after disorder averaging, they can be applied even in experiments where the disorder realization changes between individual experimental runs. This is especially important for realizations involving atoms or molecules loaded at random into a deep optical lattice; in such systems each disorder realization is destroyed upon measurement. We also emphasize that our results are obtained for the case when the effective temperature is infinite, i.e., when the energy density of the initial states is comparable to  $J_{\perp}$  and  $W$ . This should ease the

realization of our proposal, by eliminating the cooling stage of the preparation of the initial states of our system.

*Summary.*—In summary, we showed that coherent manipulation of spins can be used to probe many-body localization. In particular, the modified spin-echo protocol directly probes the characteristic slow entanglement growth in the MBL phase, and distinguishes it from the non-interacting localized phase and the delocalized phase. We demonstrated that the corresponding response function exhibits a power-law time decay, which reflects the broad distribution of time scales present in the MBL phase. The technique is robust with respect to thermal and disorder averaging, and can be implemented, using currently accessible experimental means, in ultracold atomic, molecular, and solid-state spin systems.

We thank E. Altman, Y. Bahri, I. Bloch, T. Giamarchi, D. Huse, V. Oganesyan, A. Pal, D. Pekker, and G. Refael for insightful discussions. The authors acknowledge support from the Harvard Quantum Optics Center, Harvard-MIT CUA, the DARPA OLE program, AFOSR Quantum Simulation MURI, ARO-MURI on Atomtronics, the ARO-MURI Quism program, the Austrian Science Fund (FWF) Project No. J 3361-N20, NSERC grant, and Sloan Research Fellowship. Simulations presented in this article were performed on computational resources supported by the High Performance Computing Center (PICSciE) at Princeton University and the Research Computing Center at Harvard University. Research at Perimeter Institute was supported by the Government of Canada and by the Province of Ontario.

M. S., M. K., and S. G. contributed equally to this work.

- 
- [1] D. Basko, I. Aleiner, and B. Altshuler, *Ann. Phys. (Berlin)* **321**, 1126 (2006).
- [2] I. V. Gornyi, A. D. Mirlin, and D. G. Polyakov, *Phys. Rev. Lett.* **95**, 206603 (2005).
- [3] V. Oganesyan and D. A. Huse, *Phys. Rev. B* **75**, 155111 (2007).
- [4] M. Žnidarič, T. Prosen, and P. Prelovšek, *Phys. Rev. B* **77**, 064426 (2008).
- [5] C. Monthus and T. Garel, *Phys. Rev. B* **81**, 134202 (2010).
- [6] A. Pal and D. A. Huse, *Phys. Rev. B* **82**, 174411 (2010).
- [7] E. Cuevas, M. Feigel'man, L. Ioffe, and M. Mezard, *Nat. Commun.* **3**, 1128 (2012).
- [8] J. H. Bardarson, F. Pollmann, and J. E. Moore, *Phys. Rev. Lett.* **109**, 017202 (2012).
- [9] R. Vosk and E. Altman, *Phys. Rev. Lett.* **110**, 067204 (2013).
- [10] S. Iyer, V. Oganesyan, G. Refael, and D. A. Huse, *Phys. Rev. B* **87**, 134202 (2013).
- [11] M. Serbyn, Z. Papić, and D. A. Abanin, *Phys. Rev. Lett.* **110**, 260601 (2013).
- [12] M. Serbyn, Z. Papić, and D. A. Abanin, *Phys. Rev. Lett.* **111**, 127201 (2013).
- [13] D. A. Huse and V. Oganesyan, [arXiv:1305.4915](https://arxiv.org/abs/1305.4915).
- [14] D. A. Huse, R. Nandkishore, V. Oganesyan, A. Pal, and S. L. Sondhi, *Phys. Rev. B* **88**, 014206 (2013).
- [15] B. Bauer and C. Nayak, *J. Stat. Mech.* (2013) P09005.
- [16] B. Swingle, [arXiv:1307.0507](https://arxiv.org/abs/1307.0507).
- [17] D. Pekker, G. Refael, E. Altman, and E. Demler, *Phys. Rev. X* **4**, 011052 (2014).
- [18] R. Vosk and E. Altman, *Phys. Rev. Lett.* **112**, 217204 (2014).
- [19] Y. Bahri, R. Vosk, E. Altman, and A. Vishwanath, [arXiv:1307.4092](https://arxiv.org/abs/1307.4092).
- [20] A. Chandran, V. Khemani, C. R. Laumann, and S. L. Sondhi, *Phys. Rev. B* **89**, 144201 (2014).
- [21] R. Nandkishore, S. Gopalakrishnan, and D. A. Huse, *Phys. Rev. B* **90**, 064203 (2014).
- [22] M. Schiulaz and M. Müller, *AIP Conf. Proc.* **1610**, 11 (2014).
- [23] Z. Ovadyahu, *Phys. Rev. Lett.* **108**, 156602 (2012).
- [24] M. Pasienski, D. McKay, M. White, and B. DeMarco, *Nat. Phys.* **6**, 677 (2010).
- [25] C. D'Errico, M. Moratti, E. Lucioni, L. Tanzi, B. Deissler, and M. Inguscio, *New J. Phys.* **15**, 045007 (2013).
- [26] S. S. Kondov, W. R. McGehee, and B. DeMarco, [arXiv:1305.6072](https://arxiv.org/abs/1305.6072).
- [27] K. Ni, S. Ospelkaus, M. H. G. deMiranda, A. Pe'er, B. Neyenhuis, J. J. Zirbel, S. Kotochigova, P. S. Julienne, D. S. Jin, and J. Ye, *Science* **322**, 231 (2008).
- [28] B. Yan, S. A. Moses, B. Gadway, J. P. Covey, K. R. A. Hazzard, A. M. Rey, D. S. Jin, and J. Ye, *Nature (London)* **501**, 521 (2013).
- [29] M. W. Doherty, N. B. Manson, P. Delaney, F. Jelezko, J. Wrachtrup, and L. C. L. Hollenberg, *Phys. Rep.* **528**, 1 (2013).
- [30] L. M. K. Vandersypen and I. L. Chuang, *Rev. Mod. Phys.* **76**, 1037 (2005).
- [31] O. Mandel, M. Greiner, A. Widera, T. Rom, T. W. Hänsch, and I. Bloch, *Phys. Rev. Lett.* **91**, 010407 (2003).
- [32] J. Guzman, G.-B. Jo, A. N. Wenz, K. W. Murch, C. K. Thomas, and D. M. Stamper-Kurn, *Phys. Rev. A* **84**, 063625 (2011).
- [33] M. Knap, A. Shashi, Y. Nishida, A. Imambekov, D. A. Abanin, and E. Demler, *Phys. Rev. X* **2**, 041020 (2012).
- [34] M. Knap, A. Kantian, T. Giamarchi, I. Bloch, M. D. Lukin, and E. Demler, *Phys. Rev. Lett.* **111**, 147205 (2013).
- [35] P.-K. Wang, C. P. Slichter, and J. H. Sinfelt, *Phys. Rev. Lett.* **53**, 82 (1984).
- [36] A. Milov, A. Ponomarev, and Y. Tsvetkov, *Chem. Phys. Lett.* **110**, 67 (1984).
- [37] R. G. Larsen and D. J. Singel, *J. Chem. Phys.* **98**, 5134 (1993).
- [38] See Supplemental Material at <http://link.aps.org/supplemental/10.1103/PhysRevLett.113.147204> for more details on the effect of higher-spin interactions and the DEER response for initial product states.
- [39] Spin echo was implemented using both the protocol of Fig. 1(b) and a modified protocol in which a  $\pi/2$  pulse was applied to region II at time  $t = 0$ ; the disorder-averaged fidelity shows the same behavior for both protocols.
- [40] N. Strohmaier, D. Greif, R. Jördens, L. Tarruell, H. Moritz, T. Esslinger, R. Sensarma, D. Pekker, E. Altman, and E. Demler, *Phys. Rev. Lett.* **104**, 080401 (2010).
- [41] S. Trotzky, P. Cheinet, S. Fölling, M. Feld, U. Schnorrberger, A. M. Rey, A. Polkovnikov, E. A. Demler, M. D. Lukin, and I. Bloch, *Science* **319**, 295 (2008).
- [42] T. Fukuhara, A. Kantian, M. Endres, M. Cheneau, P. Schau, S. Hild, D. Bellem, U. Schollwöck, T. Giamarchi, C. Gross, I. Bloch, and S. Kuhr, *Nat. Phys.* **9**, 235 (2013).
- [43] L. S. Levitov, *Phys. Rev. Lett.* **64**, 547 (1990).
- [44] A. L. Burin, [arXiv:cond-mat/0611387](https://arxiv.org/abs/cond-mat/0611387).
- [45] N. Y. Yao, C. R. Laumann, S. Gopalakrishnan, M. Knap, M. Mueller, E. A. Demler, and M. D. Lukin, [arXiv:1311.7151](https://arxiv.org/abs/1311.7151).